Virchows Arch. A Path. Anat. and Histol. 362, 207—221 (1974)

Ultrastructure of Muscle in Stiff-Man Syndrome

R. Yarom, J. Chaco, and D. Steigbuegel

Department of Pathology, Internal Medicine A and Physical Medicine and Rehabilitation, Hadassah Medical School-Hebrew University, Jerusalem, Israel

Received September 11, 1973

Summary. Ultrastructural changes observed in a muscle biopsy from a patient suffering with "Stiff-man" syndrome are described. In addition to nonspecific degenerative and regenerative changes in the myofibers, the site of maximal pathology seems to be the myoneural junction, with mainly hypertrophic and hyperplastic changes of the motor end plates. The possible pathophysiological factors causing these inductive changes are discussed.

Introduction

Stiff-man syndrome is a vague condition for which the diagnostic criteria include: 1) generalized muscular stiffness, disappearing during sleep; 2) normal neurological examination; 3) continual EMG activity at rest; 4) depression of EMG activity and muscle stiffness with general anaesthesia, spinal anaesthesia, peripheral blockade and curare [6, 7, 17]. The disease progresses slowly for months or years with attacks of painful, prolonged cramps and spasms superimposed on general muscle stiffness. It resembles subacute or chronic recurrent tetanus.

The etiology is thought to be central. To explain the muscle rigidity, it was suggested [6] that the fusimotor system is involved and that the activity of motor neurons becomes unduly influenced by drives from suprasegmental regions. The post synaptic potentials are abolished, so that there is no inhibition (through activity of spinal interneurons) of impulses coming from higher centers. It is also possible that more than one etiological factor is responsible for the syndrome [6, 7].

No characteristic cellular lesion has been described in the stiff-man syndrome. Muscle biopsy usually reveals normal histology, although there is a report of some degenerative and regenerative changes, cellular infiltration and proliferation of connective tissue [6]. The question was raised as to whether the above changes might not have been caused by the trauma and ischemia associated with the spasms [6].

The present report describes the abundant subcellular changes found in a histologically unremarkable muscle biopsy from a patient with stiff-man syndrome. To the best of our knowledge, there have been no previous reports of the ultrastructure of muscles and neuromuscular junctions in this condition.

This work was supported in part by a grant from the joint Research Fund of the Hebrew University-Hadassah Medical School.

Materials and Methods

Short Clinical History

At the time of the examination, the patient was a 29-year old merchant, married, with three children. He was well until 7 years previously when painful muscle cramps and stiffness developed. Various groups of muscle fibers contracted forcibly and painfully for a few seconds at a time. These attacks lasted minutes to hours and recurred at first every few weeks and finally every few days. There were no attacks at night and sleep was never disturbed. The patient had been hospitalized several times, and numerous laboratory and electrodiagnostic tests, as well as a muscle biopsy had been done, but had failed to establish a diagnosis. During the 4 years before the present admission, he had also been suffering from ulcerative colitis, as confirmed by typical intestinal x-ray findings and a rectal biopsy. There had been a vague history of epileptic fits 4 years previously, completely controlled by phenobarbitone which he continued to take. The patient was admitted to the hospital six weeks before the examination because of exacerbation of both the muscle condition and the colitis. A severe attack soon after admission was accompanied by bronchospasms and required curarization for relief.

Physical examination revealed widespread intermittent cramps shifting from one muscle group to another. Neurological examination revealed no abnormal findings(!). The only abnormality in the laboratory tests consisted of increased serum globulin (total proteins 6.9 g-%, albumen to globulin ratio, 2.8:4.1) and on electrophoresis the gamma globulin fraction was 25.6%. The EMG showed multiple potentials from deltoid muscles during rest. Each potential was normal with an amplitude of 600 microvolts and duration of 3 milliseconds. When the same procedure was done in the absence of cramps, action potentials still registered on the oscilloscope, although these were less numerous. EEG showed an abnormal nonspecific record with no localized epileptic focus.

The patient had been receiving the following drugs: salazopyrine, 5 gm daily, and phenobarbitone, 100 mg daily, for 4 years; ACTH, 20 units per day for 8 days, 2 months before the examination, followed by meticorten, 40 mg per day for 7 weeks; finally diazepam (valium), 40 mg per day for 6 weeks with good effect. The patient left the hospital markedly improved, but not completely free from the stiffness or attacks of cramps.

Muscle Tissue Biopsy and Preparation for Electron Microscopy

An open biopsy from the deltoid muscle was performed in the operating theater. 1% Lignocaine was used and care taken to anaesthesize the skin only and not the underlying muscle. A "no touch" technique was employed as far as possible. Three pieces of tissue, each about 1 cm long and 0.3 cm thick, were removed after tying ligatures at the two ends of each sample. The pieces were fixed in a slightly stretched state by first dripping fixative onto the secured tissue, and then by an additional hour's immersion in cold fixative. The fixative solutions were a) 3% glutaraldehyde buffered with 0.1 M Na cacodylate and post-fixed in osmium tetroxide, b) 2% osmium tetroxide with the same buffer, or c) 2% potassium pyroantimonate with 1% osmium tetroxide dissolved in 0.01 N acetic acid, unbuffered [18]. All the samples were dehydrated in graded alcohols, followed by propylene oxide and embedding in Epon 812. Thin sections were cut onto 200 and 300 mesh formvar-coated copper grids. These were stained with uranyl acetate and lead citrate and viewed with a Philips 300 electron microscope.

To compare the potassium pyroantimonate fixation with controls, samples of two normal muscles were taken in a similar manner during open surgery for unrelated conditions, and prepared as described above.

Observations

Change in Muscle Fiber

Twenty different tissue blocks from material in the three fixative mixtures were examined in the phase and electron microscopes. Many myofibers appeared quite normal and the only abnormality in some was an overabundance of glycogen (Figs. 1, 2). In several areas where red and white fibers were seen together, the

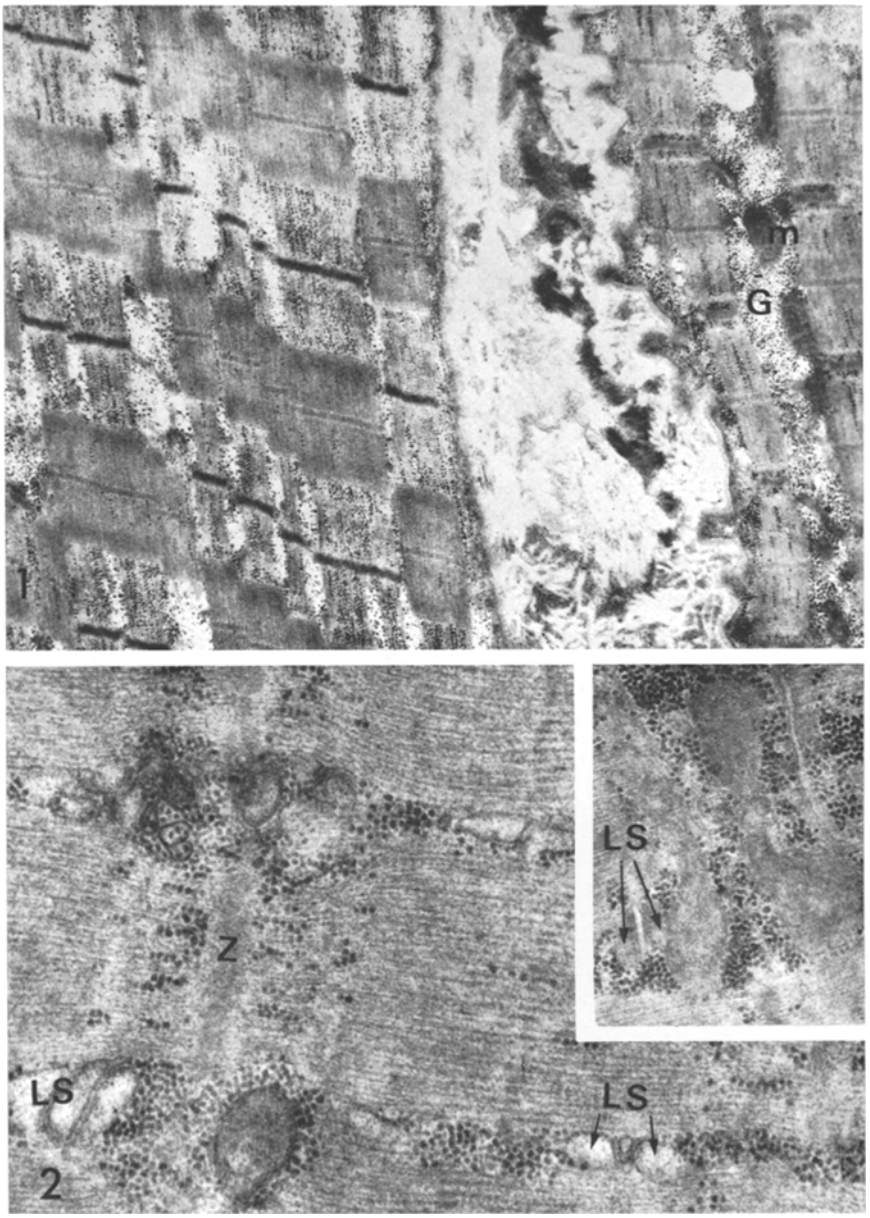

Fig. 1. Two adjacent, glycogen-rich muscle cells. The myofiber on the right is probably a red fiber with numerous mitochondria (*m*); it is contracted and contains an excessive amount of glycogen (*G*). The myofiber on the left is probably a white fiber; it appears relaxed and stretched (sarcomere length approximately 3.6 μ). (×11200)

Fig. 2. Myofiber fixed in osmium shows triads with apparently empty slightly dilated lateral sacs (*LS*). Insert: when the muscle is fixed with glutaraldehyde, sacs appear normal and contain granular material. (×35000, insert ×26000)

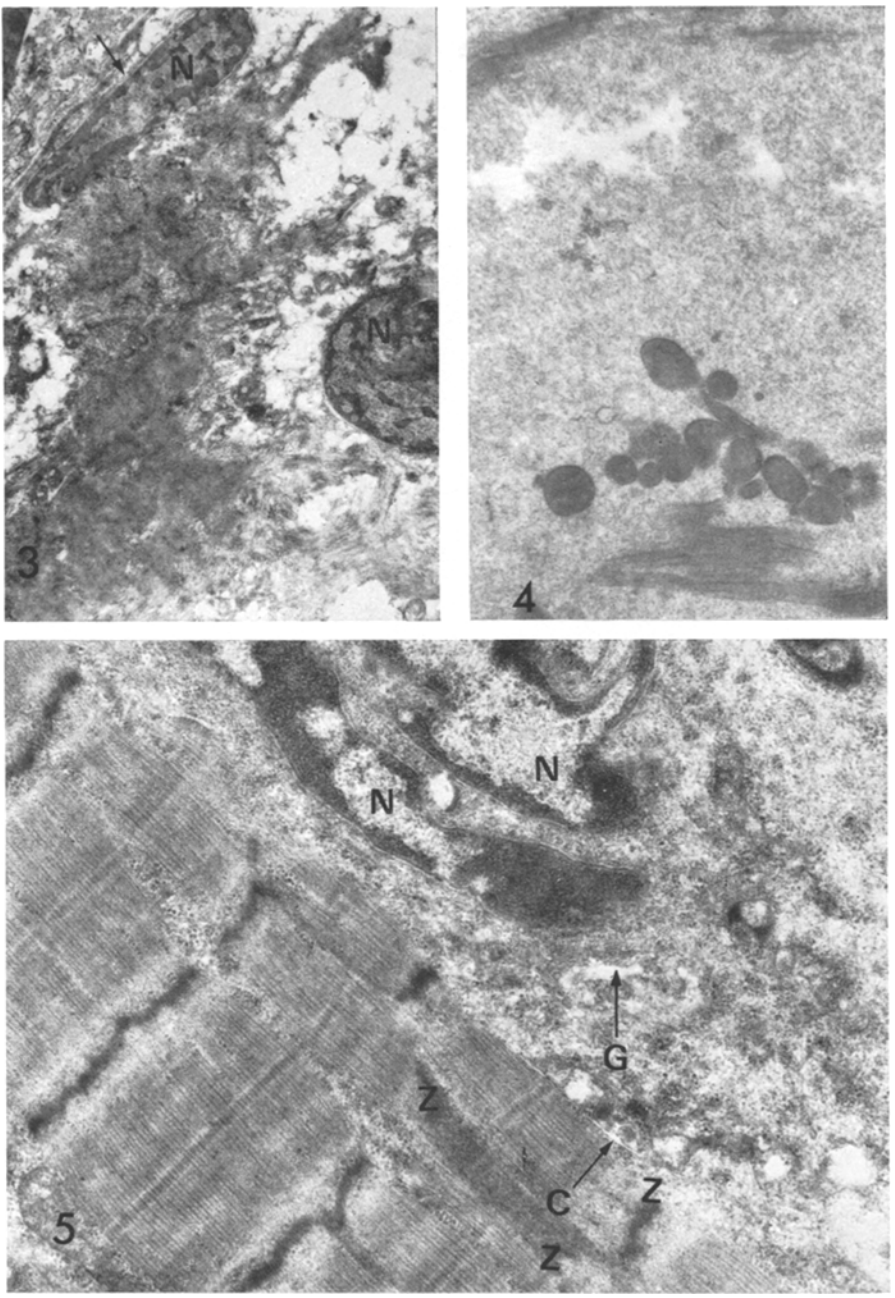

Fig. 3. Structureless myofiber shaving preserved basement membrane (arrow), and two nuclei (*N*) with clumped marginal chromatin. Sarcoplasm contains large vacuoles, fibrillar and amorphous material. (×5600)

Fig. 4. Degenerated myofiber seen with remnants of mitochondria and myofilaments in a granular matrix. (×9000)

Fig. 5. Margin of myofiber with an indented nucleus. Parts of the nuclear envelope are ill-defined; nearby is a Golgi apparatus (*G*). The sarcoplasm is partly separated from the myofilaments by a cleft (*C*). The Z lines (*Z*) are thick, distorted and "streaming" with occasional deposition of electron dense material. (×25000)

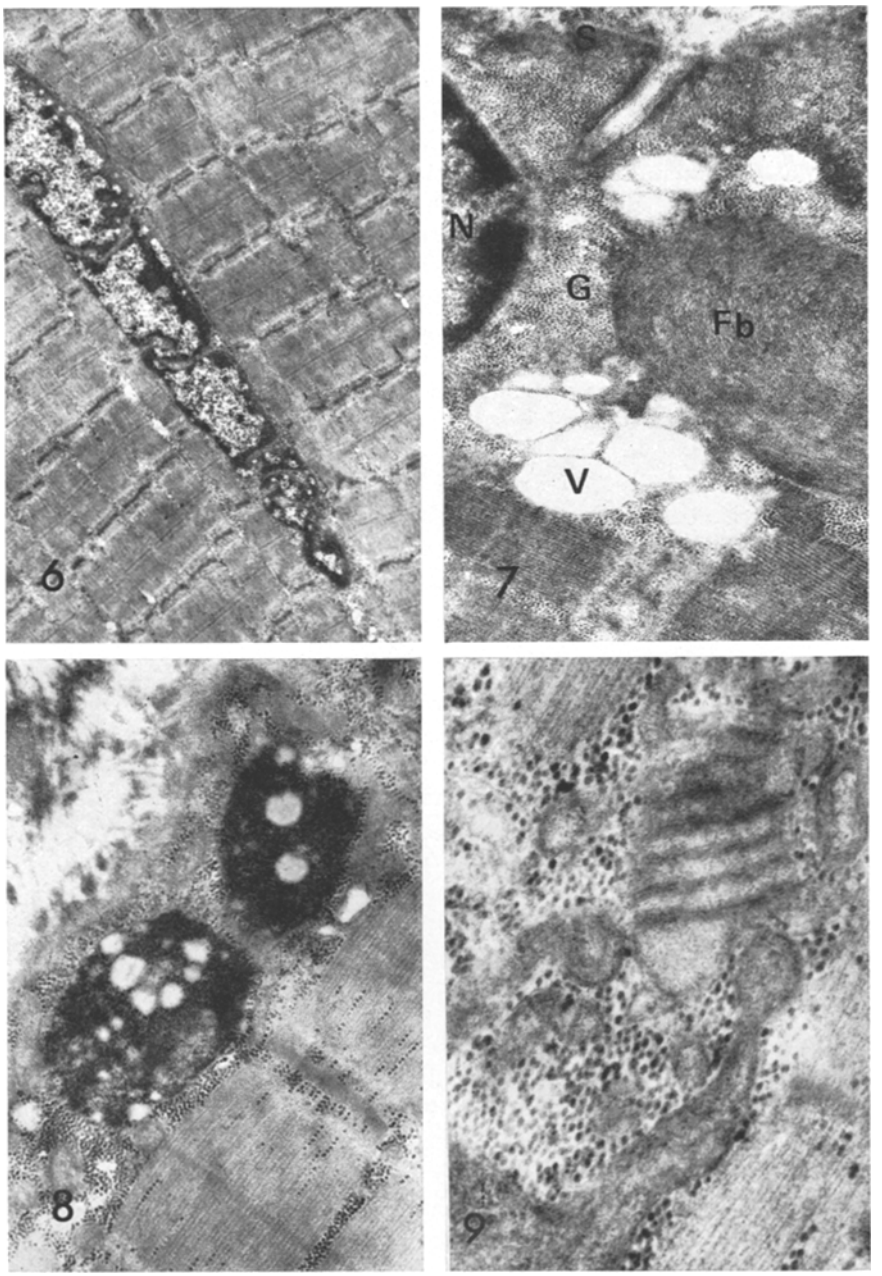

Fig. 6. Muscle fiber with central elongated, tortuous myonucleus. (×2500)

Fig. 7. Muscle fiber showing filamentous body (*Fb*) and large vacuoles (*V*). Myonucleus (*N*), sarcolemma (*S*) and large amount of glycogen can be seen. (×30000)

Fig. 8. Two lipid bodies located near sarcolemma. (×20000)

Fig. 9. Appearance of pyramidal body. (×40000)

red (containing many mitochondria) appeared much more contracted and contained more glycogen. Ultrastructural changes occured focally and were easily found on every grid examined. The myofilaments showed areas of disorganization and frank degeneration, usually near the sarcolemma (Figs. 3, 4). There was frequent "streaming", thickening and zigzaging of the Z lines with deposition of electron-dense material in some sarcomeres (Fig. 5). The sarcoplasmic reticulum could not be visualized well, but the triads were quite prominent and appeared unchanged (Fig. 2). The mitochondria were inconspicuous and both small dark and pale dilated forms could be seen. The myonuclei were very striking. They were often very long, snakelike and tortuous with abundant dark marginal chromatin and one or more nucleoli. Central myonuclei, sometimes multiple and arranged in a row were found (Fig. 14). The perinuclear sarcoplasm was rich in ribosomes and glycogen and contained prominent Golgi apparatus, vesicles, vacuoles, lipid bodies, tubular, filamentous and concentric laminar bodies (Figs. 5, 7–9).

In the interstitial spaces there were capillaries with large pericytes, poorly preserved nerves and many cells with long narrow processes (Figs. 10, 11). There were also many collagen fibrils and folded congregations of basement membranelike material (Fig. 11). Definite satellite cells were frequent (Fig. 10).

Myoneural Junctions

Motor end plates were found in several tissue sections, Changes of similar nature but of varying degree were observed in most of them and consisted mainly of proliferation and hypertrophy (Figs. 12–17). The junctional sarcoplasm was abundant and contained one or more nuclei, as well as granular and vesicular material, but no other formed organelles. The primary synaptic clefts (gutters) were deep and often multiple, arranged one next to another along the myofiber. Papillary projections and overhanging folds occurred (Figs. 14, 15). The secondary clefts and folds were overabundant, complex and narrow. On the inner aspect of the postsynaptic membranes, electron dense material often accumulated; within the fold, basement membranelike material could be discerned (Figs. 13, 16). In the deeper layers and at the margins of the primary gutters the secondary folds were often disorganized. In several sections the sarcoplasm adjacent to the myonuclei (even when these were centrally placed) was especially rich in granular material and contained structures definitely resembling secondary synaptic folds

Fig. 10. Edges of two muscle cells showing details of interstitial space which contains two oblong cells with long narrow processes (*P*). A satellite cell nucleus is seen intimately related to the lower myofiber. Near it is seen undulating sarcolemma. The upper fiber has complicated indented and oblong nuclei (*N*). On left is seen junctional sarcoplasm near a motor end plate containing granular material and structures resembling secondary synaptic folds (arrow). (×5000)

Fig. 11. Edge of myofiber with nearby long cytoplasmic cell processes containing intracellular tubular structures (arrow). Also indicated are laminated basement membranelike material (*Bm*), and ill-defined Z line (*Z*). (×40000)

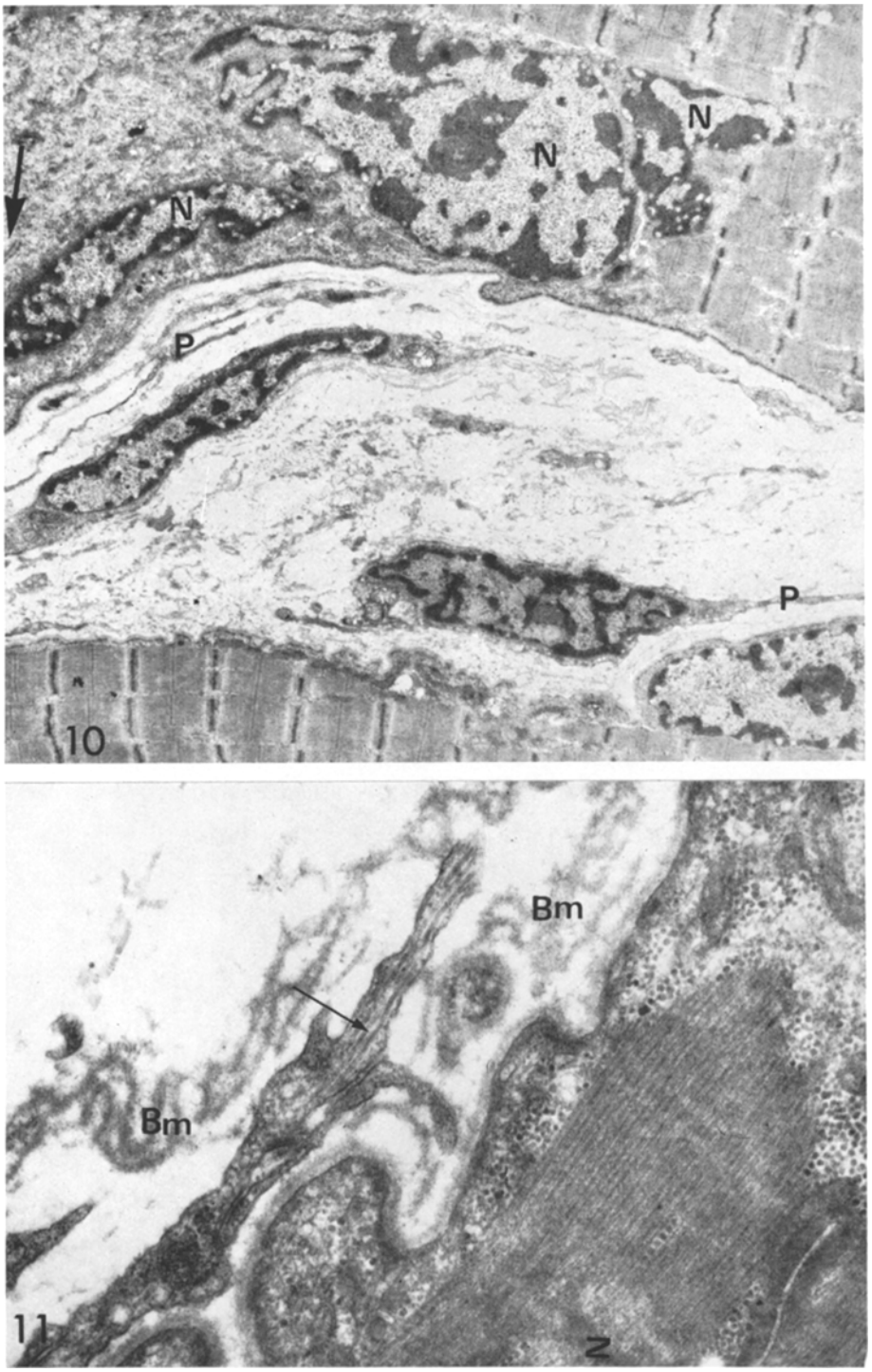

Figs. 10 and 11

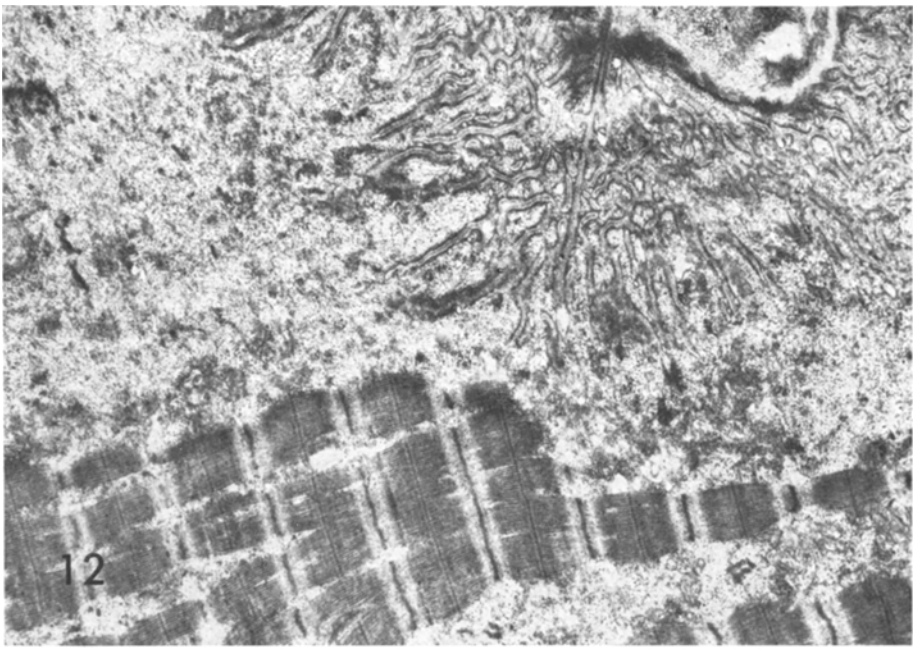

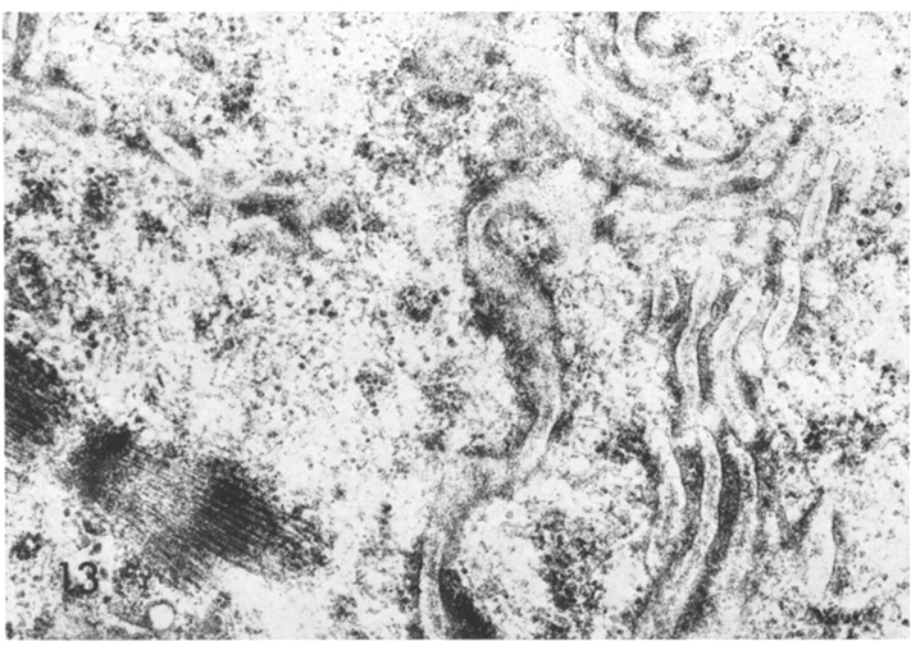

Fig. 12. Motor end plate of muscle fiber. The primary synaptic cleft at upper right contains a poorly preserved terminal axon with synaptic vesicles. The secondary synaptic folds are abundant, narrow and branching. The junctional sarcoplasm contains granular material and lacks mitochondria. Underlying myofibers show degenerative (or regenerative) changes. ($\times 7000$)

Fig. 13. Enlargement of lower right-hand part of Fig. 12. Structures resembling secondary synaptic folds are abundant within the granular sarcoplasm. Part of a myofibril is seen at the lower left. ($\times 35000$)

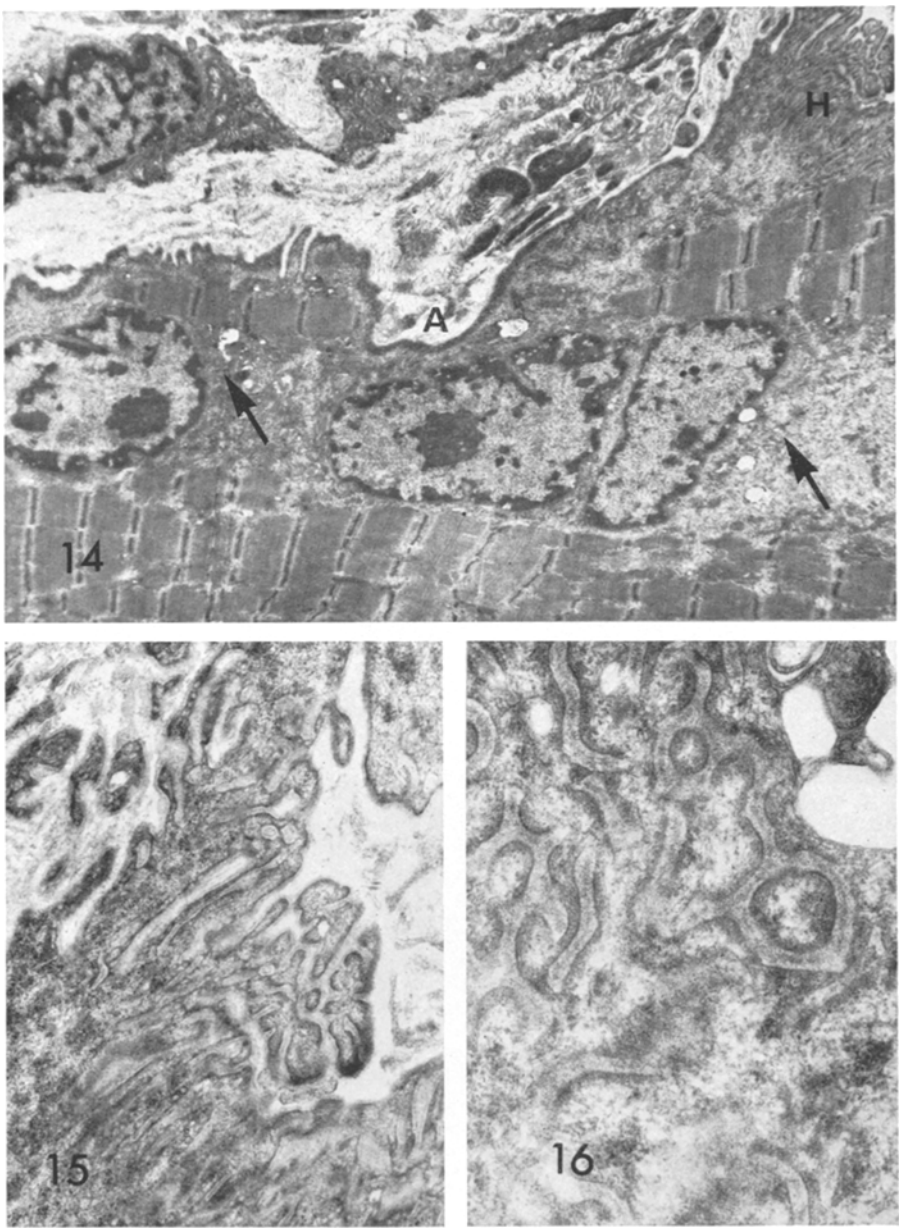

Fig. 14. Muscle fiber showing three nuclei with prominent nucleoli. The perinuclear and subsarcolemmal sarcoplasm is granular and contains structures resembling secondary synaptic folds (arrows, enlargement of area near left arrow is seen in Fig. 16). The sarcolemma is thrown into irregular folds. Atrophic (*A*) and hypertrophic (*H*) primary gutters appear. A degenerating structure of uncertain origin (perhaps a nerve or a muscle spindle ?) is seen in the interstitial tissue. (×3600)

Fig. 15. Enlargement of area (*H*) in Fig. 14 showing hypertrophied motor end plate with overhanging papillary-like projections consisting of secondary synaptic folds. Only ill-defined materials is found in the primary groove. (×10000)

Fig. 16. Enlargement of area near left hand arrow of Fig. 14 showing branching structures resembling secondary synaptic folds. (×30000)

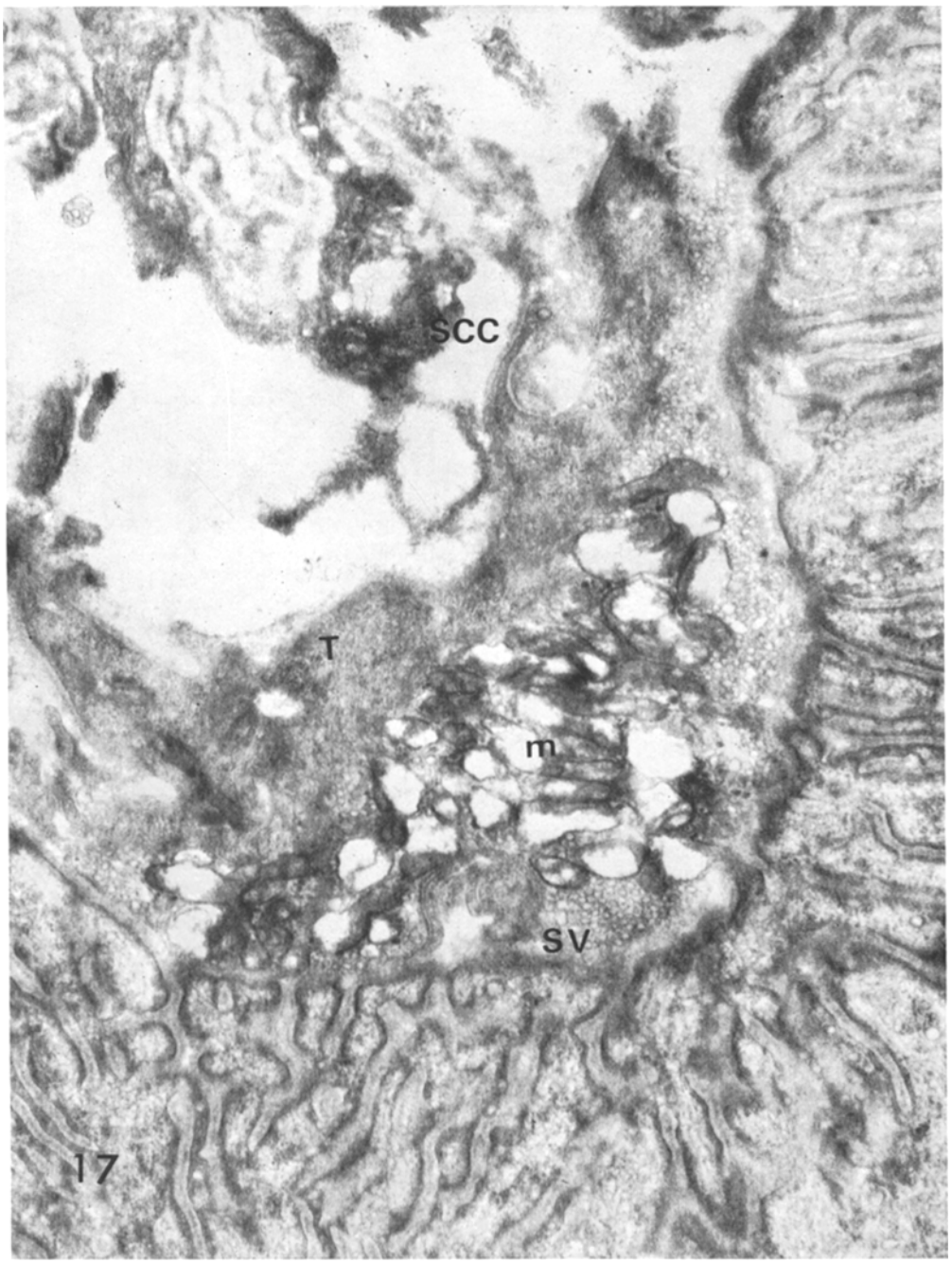

Fig. 17. Hypertrophied myoneural junction. A nerve terminal is discerned in the primary cleft. Preservation is poor and mitochondria (*m*) are ballooned. Numerous small synaptic vesicles (*SV*) and perhaps tubular structures (*T*) are seen. The Schwann cell cytoplasm (*SCC*) is ill-defined. (×21000)

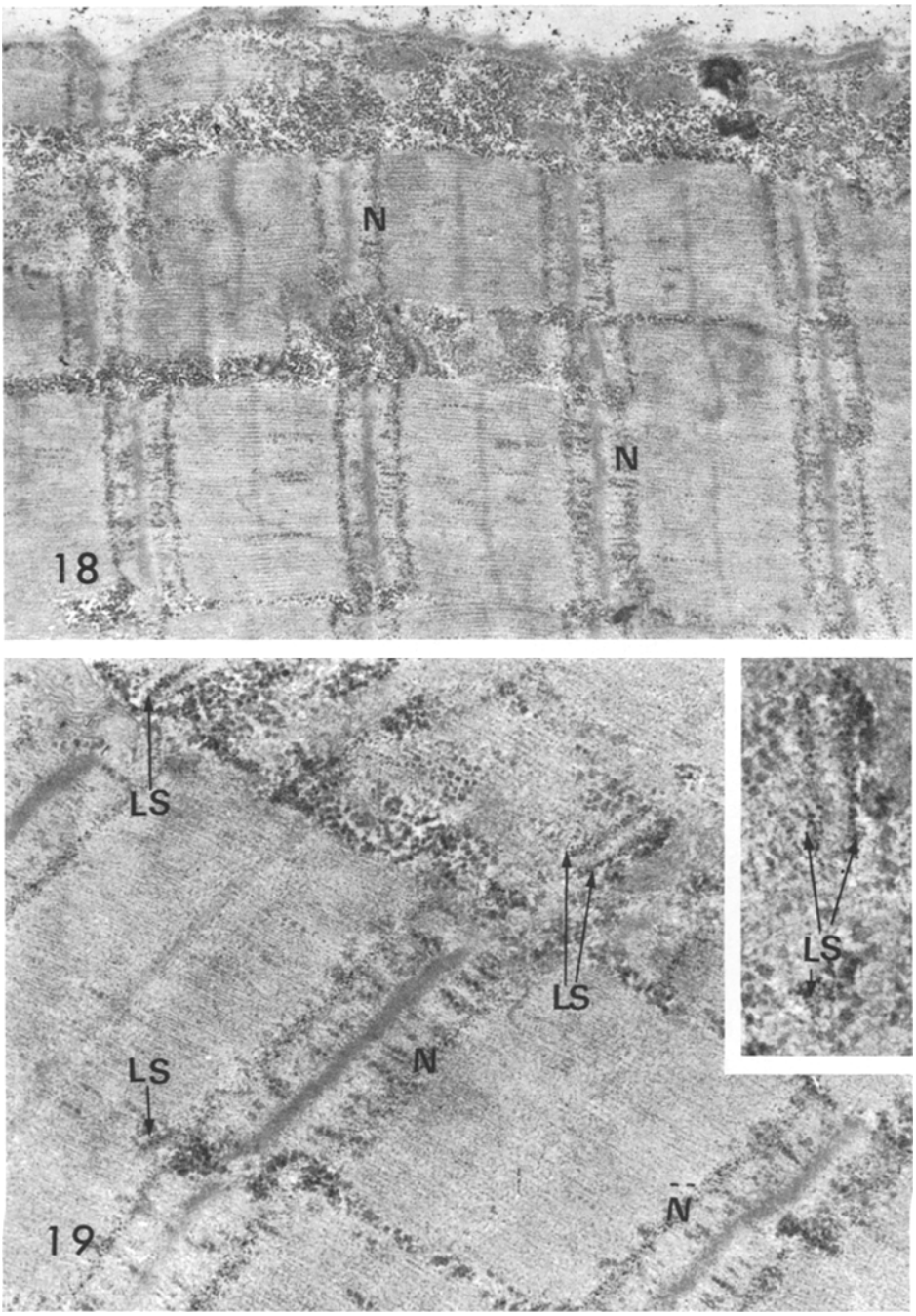

Fig. 18. Muscle fixed in Potassium pyroantimonate and osmium mixture. There is a normal distribution of calcium, the precipitate concentrating on the N line of the I bands (*N*) and in the Lateral sacs. A large amount of glycogen is present in the interfibrillary fibrillary spaces. (×15000)

Fig. 19. Muscle fixed as above. The calcium precipitate is scanty but obvious as a linear accumulation across the thin filaments and is the lateral sacs (arrows) (glycogen granules are larger and less electron dense). (×30000). Insert shows higher magnification of triad. (×60000)

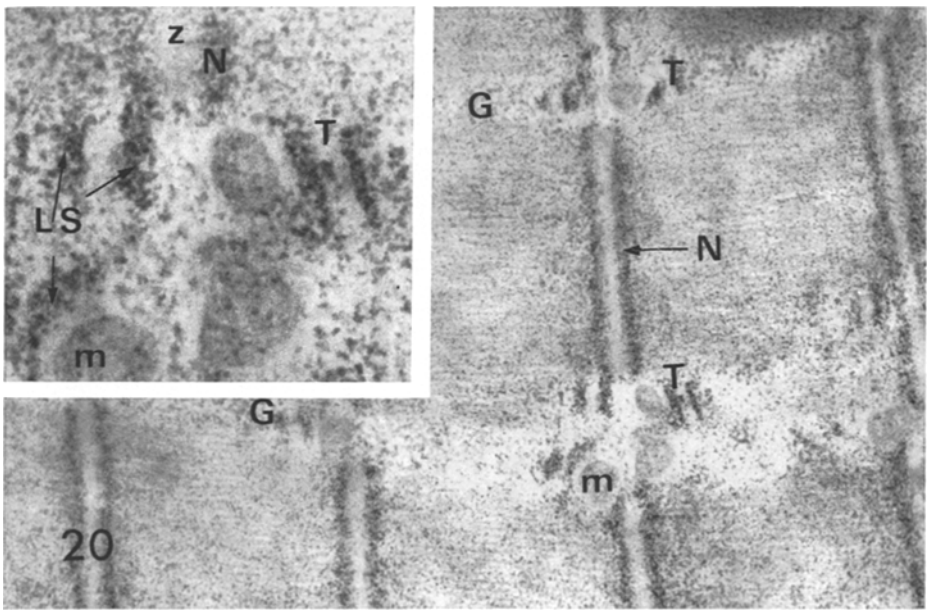

Fig. 20. Normal muscle from a control case, fixed with pyroantimonate and osmium, unstained. There is abundant precipitate in the contracted sarcomeres, mainly near the Z lines (*N*) and in the lateral sacs (*LS*) of the triads (*T*). Glycogen granules (*G*) are larger and paler than the calcium antimonate deposits. *m* mitochondria. (×26000), (×80000)

(Figs. 14, 16). Underlying and neighboring myofibrils were normal or showed some disorganization and degeneration. Terminal axons were seen within the primary gutters, covered on one side by a Schwann cell (Fig. 17). The state of preservation of the nerve endings was not good. The mitochondria were ballooned and structureless cysts occurred. The synaptic vesicles appeared small and numerous, and often arranged in clumps. The plasma membranes of axons and Schwann cells were ill-defined and often missing. The part of the muscle which was fixed in the pyroantimonate and osmium mixture showed no Ca localisation which differed significantly from the normal controls.

A fine precipitate accumulated along the N lines of the thin filaments and in the lateral sacs of the triads, as well as in the nuclei and the interfibrillary spaces (Figs. 18–20) [18]. In most areas but especially in the lateral sacs, the deposits appeared to be less abundant than in the 2 normal controls. The myoneural junctions were poorly visualized with the pyroantimonate method.

Discussion

This report reveals hitherto unsuspected ultrastructural pathology of muscle, motor end plates, and terminal nerves in a case of stiff-man syndrome. Although the clinical criteria for including this case in the syndrome have been met, the patient's history is complicated with an associated serious illness and the many drugs used in therapy. The role played by all these factors in the muscle pathology

is not certain. Although the morphological changes appear to be especially severe at the neuromuscular junctions, these do not offer a clear explanation of the etiology and pathogenesis of the syndrome. Indeed, it is becoming more and more evident that definite structure-function-injury correlations are impossible to demonstrate in many muscle diseases. The problem of primary myogenic or primary neurogenic injury is complex; traditional concepts are being challenged and many primary myopathies are now thought to have a neural basis [5]. Examination of tissues in neurogenic diseases and in experiments with denervation as a rule show severe morphological, as well as physiological changes in muscles. Degenerative and regenerative processes occur together and the responses of the two muscle fiber types may differ [5, 8, 9, 12, 16]. Muscle pathology is thus rarely clear-cut or specific, and many similar changes have been described in different diseases.

In this case, many features of injury to muscle were found. There were changes in the myofilaments, such as frank atrophy, Z line abnormalities, accumulation of electron-dense filamentous and amorphous material. The nuclei showed elongation, tortuosity, changes in position and number. There were excessive ribosomes, glycogen, lipid, degenerative bodies, and amorphous material in the sarcoplasm and, finally, the number of interstitial cells associated with the sarcolemma was high. However, the motor end plate pathology appears to be most important and is perhaps directly related to the clinical manifestations of the syndrome.

There are few reports of ultrastructural pathology in human neuromuscular junctions. Normal motor end plates vary according to myofiber type, being shallow and sparse in red fibers, long and branching in white ones [3, 10, 14]. In diseased states the diversity of structure may become obliterated so that only an experienced observer can diagnose morphological abnormality. Several reports describe junctional pathology. In myasthenia gravis there is a decrease in number, size and depth of primary synaptic clefts, while the secondary folds are wide, short and few [2, 14]. In tetanus, which clinically resembles the stiff-man syndrome, no pathology is found in the neuromuscular junctions [1, 19]. On the other hand, ultrastructural changes resembling those observed here have been noted after treatment with cholinesterase inhibitors [4, 14], in muscular dystrophy, polymyositis [16] and in the myasthenic syndrome [15]. The latter is a condition, sometimes associated with bronchogenic carcinoma, which resembles myasthenia gravis. However, its subcellular pathology shows motor end plate proliferation and hypertrophy.

Histometric methods [14, 15] have been used to demonstrate more definitely the neuromuscular junction aberrations. These methods produce quantitative ratios of pre- and post-synaptic areas of contact, but fail to explain the pathophysiological processes involved in the various motor end plate diseases. In our case, as in the myasthenia syndrome, the ratio of pre to post-synaptic membrane appeared very high.

Neurotransmitter substances and their quantal release mechanism are intimately related to synaptic vesicles. However, the multiple factors connected with their release, inactivation, and reuptake contribute to the difficulty in understanding the exact mechanisms involved and in demonstrating structure-

function relations. Studies of myogenesis and pathophysiology demonstrate that neurotransmitters also act as inductive agents on the post synaptic regions [11, 13, 14]. It might be possible that the proliferative motor end-plate changes observed are caused by excessive acetylcholine release due to increased descending impulses or to impairment of inhibitory pathways.

In general, muscle cramps and stiffness may be due to several factors. These include excessive descending facilitory impulses exciting alpha and gamma motor neurons, loss of inhibitory function, overactivity of nerves along all their extent, abnormalities of the muscle fiber postsynaptic membrane and finally malfunction of the intracellular contraction-relaxation coupling apparatus. In this last, the role of intracellular calcium is most important. A histochemical examination of its concentration sites as compared with normal controls could perhaps contribute towards differentiating between particular mechanisms involved in causing muscle stiffness and cramps.

The use of the pyroantimonate technique suggests that there is less calcium in sick muscle than in normal controls, especially in the lateral sacs; this may point to an insufficient calcium sequestrating system which could theoretically result in inadequate muscle relaxation, causing cramps and stiffness. However, the unpredictability of fixative penetration as well as the uncertain effects of preparatory procedures still make the pyroantimonate method too variable for even semiquantitative estimates of calcium concentrations. In conclusion, since in the case here described the effects on the neuromuscular junctions of the associated illness and drugs taken remain unknown, the ultrastructural changes observed can only allow speculation as to the possible pathogenesis of stiff-man syndrome.

We would like to thank B. Golek for the editorial help.

References

1. Agostini, B., Noetzel, H.: Morphological study of muscle fibers and motor end-plates in tetanus. Excerpta Medica International Congress Series, No 199, Muscle Diseases, Proceedings of an Intern. Congress, Milan, p. 123–127 (May 1969)
2. Anderson, P. J., Slotwiner, P.: The fine structure of spheromembranous degeneration of skeletal muscle induced by vincristine. J. Neuropath. exp. Neurol. **25**, 15–24 (1967)
3. Engel, A. G.: Locating motor end plates for electron microscopy. Mayo clin. Proc. **45**, 450 (1970)
4. Engel, A. G., Santa, T.: Effect of long-term anticholin-esterese treatment on neuromuscular transmission and on motor-end-plate fine structure. Neurology (Minneap.) **22**, 401–402 (Abst.) (1972)
5. Gallup, B., Dubowitch, V.: Failure of dystrophic neurons to support functional regeneration of normal or dystrophic muscle in culture. Nature (Lond.) **243**, 287–289 (1973)
6. Gordon, E. E., Januszko, D. M., Kaufman, L.: A critical survey of stiff-man syndrome. Amer. J. Med. **42**, 582–592 (1967)
7. Layzer, R. B., Rowland, L. P.: Cramps. New Engl. J. Med. **285**, 31–40 (1971)
8. Mair, W. G. P., Tome, F. M. S.: Atlas of the ultrastructure of diseased human muscle. Edinburgh-London: Churchill Livingstone 1972
9. Miledi, R., Slater, C. R.: Electron microscopic structure of denervated skeletal muscle. Proc. roy. Soc. B **174**, 253–269 (1969)
10. Padykula, H. A., Gauthier, G. F.: The ultrastructure of the neuromuscular junction of mamalian red, white and intermediate skeletal muscle fibers. J. Cell Biol. **46**, 24 (1970)

11. Pysh, J. J., Wiley, R. G.: Morphologic alterations of synapses in electrically stimulated cervical ganglia of the cat. Science **176**, 191–193 (1972)
12. Romanul, F. C. A., Meulen, J. P. van der: Slow and fast muscles after cross innervation. Arch. Neurol. (Chic.) **17**, 387–402 (1967)
13. Saito, A., Zacks, S. I.: The fine structure of motor-end plate morphogenesis. J. Cell Biol. **42**, 154 (1969)
14. Santa, T., Engel, A. G., Lambert, E. H.: Histometric study of neuromuscular junction ultrastructure. I. Myesthenia Gravis. Neurology (Minneap.) **22**, 71–82 (1972)
15. Santa, T., Engel, A. G., Lambert, E. H.: Histometric study of neuromuscular junction ultrastructure, II. Myesthenic syndrome. Neurology (Minneap.) **22**, 370–376 (1972)
16. Song, S. K.: Electron microscopic study of terminal nerves, motor-end plates and sarcoplasmic structures in denervated skeletal muscle. J. Neuropath. exp. Neurol. **27**, 108 (Abstr.) (1968)
17. Wallis, W. E., Poznak, A. van, Plum, F.: Generalized muscular stiffness, fasciculation and myokymia of peripheral nerve origin. Arch. Neurol. (Chic.) **22**, 430–439 (1970)
18. Yarom, R., Meiri, U.: Pyroantimonate precipitates in frogskeletal muscle. Changes produced by alterations in composition of bathing fluid. J. Histol. Cytol. **21**, 146–154 (1973)
19. Zacks, S. J., Sheff, M. F.: Tetanus toxin fine structure localization of binding sites in striated muscle. Science **159**, 643 (1968)

Dr. R. Yarom
The Hebrew University
Hadassah Medical School
Department of Pathology
P.O. Box 1172
Jerusalem
Israel